Performance Analysis of MIMO-OTFS with Decode and Forward Relaying

Vighnesh S Bhat and A. Chockalingam

Department of ECE, Indian Institute of Science, Bangalore 560012

Abstract—In this paper, we analyze the performance of multiple-input multiple-output orthogonal time frequency space (MIMO-OTFS) modulation with decode and forward (DaF) relaying. Communication between the transmitter and receiver nodes happens through a relay node in two hops. All the nodes are provided with multiple transmit and multiple receive antennas. We derive a closed-form expression for the end-to-end pairwise error probability in MIMO-OTFS with DaF relaying and characterize the achieved asymptotic diversity order. We also investigate the considered system when phase rotation of OTFS frames is performed to improve the diversity performance. Simulation results are shown to validate the analytically predicted diversity performance.

Index Terms—OTFS modulation, MIMO-OTFS, decode and forward relaying, pairwise error probability, diversity analysis.

I. INTRODUCTION

As carrier frequencies increase and high-speed use cases emerge in next generation mobile communications, modulation waveforms have to deal with high-Doppler channels which are rapidly time-varying. Orthogonal time frequency space (OTFS) modulation has been shown to offer robust performance in high-Doppler channels [1]. OTFS modulation multiplexes information symbols in the delay-Doppler (DD) domain. Several papers in the literature have examined various aspects in OTFS, such as low-complexity signal detection, DD channel estimation, peak-to-average power ratio, pulse shaping, and multiple access [2]-[5]. In terms of performance analysis of OTFS, the work reported in [6] analyzed the diversity performance of OTFS in a point-to-point setting. This study showed that the asymptotic diversity order achieved by uncoded single-input single-output OTFS is one. Also, it demonstrated that full diversity in the DD domain is achieved when phase rotation is applied to the OTFS signal vector before transmission. The diversity performance of OTFS when rectangular waveforms are used has been analyzed in [7]. Results on the achievable diversity orders in both spatial and DD domains have been reported for multiple-input multiple-output OTFS (MIMO-OTFS) and space-time coded OTFS (STC-OTFS) in [6] and [8], respectively. In [8], the performance of different multi-antenna OTFS systems with receive antenna selection are analyzed and the achievable diversity orders are derived. The error performance of coded OTFS is analyzed in [9], which shows a trade-off between the coding gain and the diversity gain in OTFS systems.

Cooperative relaying is a widely recognized means to enhance the range and coverage in wireless communications [10], [11]. Amplify-and-forward and decode-and-forward protocols are widely studied owing to their simplicity and practicality. Single-relay and multi-relay schemes without and with relay selection have been investigated in a variety of system settings [12]-[14]. The performance of cooperative communication in the presence of node mobility has been studied in [13], [14], where it has been shown that node mobility causes performance degradation. The inherent robustness of OTFS can alleviate this issue in cooperative communications with node mobility. Therefore, understanding the performance of OTFS in relaying systems in high-mobility environments is of interest. In this paper, we present an analysis of the end-to-end performance of MIMO-OTFS in decode-and-forward (DaF) relaying systems. Our contributions in this paper are as follows.

- We derive a closed-form expression for the end-to-end pairwise error probability (PEP) for MIMO-OTFS with DaF relaying, and characterize the achieved asymptotic diversity order.
- We also analyze the system when phase rotation (PR) of OTFS frames is employed to achieve improved diversity performance.
- Simulation results are shown to corroborate the analytically derived diversity orders for MIMO-OTFS with DaF relaying.

The remainder of the paper is organized as follows. The considered OTFS system model DaF relaying is presented in Sec. II. The performance analysis of this system is presented in Sec. III. Numerical results and discussions are presented in Sec. IV. A summary of conclusions is given in Sec. V.

Notations: A matrix is denoted by uppercase boldface letter, a vector by lowercase boldface letter, a diagonal matrix with entries $\{x_1, \cdots, x_n\}$ by $\text{diag}\{x_1, \cdots, x_n\}$, and Frobenius norm of matrix $\mathbf{X}$ by $\|\mathbf{X}\|$. $(\cdot)^T$, $(\cdot)^H$, $(\cdot)^*$ denote transposition, Hermitian, and conjugation operators, respectively. A complex Gaussian distribution with mean a and variance b is denoted by $\mathcal{CN}(a, b)$. Expectation operation is denoted by $\mathbb{E}[\cdot]$. $|.|$ denotes absolute value of a number or cardinality of a set.

II. SYSTEM MODEL

The OTFS modulation and demodulation consist of 2D transforms at the transmitter and the receiver. MN information

symbols, $y[k,l]$, $k = 0, \cdots, N-1$, $l = 0, \cdots, M-1$, are multiplexed over a $N \times M$ DD grid, given by $\{(\frac{k}{NT}, \frac{l}{M\Delta f}), k = 0, \cdots, N-1, l = 0, \cdots, M-1\}$, where M and N are the number of delay and Doppler bins, respectively, and $\frac{1}{M\Delta f}$ and $\frac{1}{NT}$ are the delay and Doppler bin sizes, respectively. The information symbols in the DD domain are mapped to the TF domain using inverse symplectic finite Fourier transform (ISFFT) and windowing. The TF symbols are converted to time domain using Heisenberg transform for transmission over the channel. The transmit time domain signal $y(t)$ is given by

$$y(t) = \sum_{n=0}^{N-1} \sum_{m=0}^{M-1} Y[n,m]g_{tx}(t - nT)e^{j2\pi m\Delta f(t - nT)}, \quad (1)$$

where $Y[n,m]$ is the TF domain signal at the output of ISFFT, given by

$$Y[n,m] = \frac{1}{\sqrt{MN}} \sum_{k=0}^{N-1} \sum_{l=0}^{M-1} y[k,l]e^{j2\pi\left(\frac{nk}{N} - \frac{ml}{M}\right)}, \quad (2)$$

and $g_{tx}(t)$ is the transmit pulse. The transmitted signal passes through a channel whose response in the DD domain is given by

$$g(\tau, \nu) = \sum_{i=1}^{P} g_i \delta(\tau - \tau_i)\delta(\nu - \nu_i), \quad (3)$$

where g_i, τ_i, and ν_i, respectively, denote the channel gain, delay, and Doppler associated with the ith path. The received time-domain signal $z(t)$ is given by

$$z(t) = \int_{\nu} \int_{\tau} g(\tau, \nu)y(t - \tau)e^{j2\pi\nu(t - \tau)}\mathrm{d}\tau\mathrm{d}\nu + v(t), \quad (4)$$

where $v(t)$ is the additive white Gaussian noise. At the receiver, matched filtering on the received time-domain signal is performed using Wigner transform to get TF domain symbols. Finally, with windowing and symplectic finite Fourier transform (SFFT), DD symbols are obtained from the TF symbols for demodulation. The DD domain signal at the output of the SFFT can be written as [4]

$$z[k,l] = \sum_{i=1}^{P} g_i' y[(k - \beta_i)_N, (l - \alpha_i)_M] + v[k,l], \quad (5)$$

where $g_i' = g_i e^{-j2\pi\nu_i\tau_i}$, g_is are i.i.d and are distributed as $\mathcal{CN}(0, 1/P)$ with uniform scattering profile, α_i and β_i are integers corresponding to indices of delay and Doppler, respectively, for the ith path, i.e., $\tau_i \triangleq \frac{\alpha_i}{M\Delta f}$ and $\nu_i \triangleq \frac{\beta_i}{NT}$, and $v[k,l]$ is the additive white Gaussian noise. By vectorizing the input-output relation in (5), we can write [4]

$$\mathbf{z} = \mathbf{G}\mathbf{y} + \mathbf{v}, \quad (6)$$

where $\mathbf{y}, \mathbf{z}, \mathbf{v} \in \mathbb{C}^{MN \times 1}$, the $(k + Nl)$th entry of $\mathbf{y}$, $y_{k+Nl} = y[k,l]$, $k = 0, \cdots, N-1$, $l = 0, \cdots, M-1$ and $y[k,l] \in \mathbb{A}$, where $\mathbb{A}$ is the modulation alphabet (e.g., phase shift keying (PSK) or quadrature amplitude modulation (QAM)), Similarly, $z_{k+Nl} = z[k,l]$ and $v_{k+Nl} = v[k,l]$, $k = 0, \cdots, N-1, l = 0, \cdots, M-1$, and $\mathbf{G} \in \mathbb{C}^{MN \times MN}$ is the effective channel matrix, whose jth row $(j = k + Nl)$, denoted by $\mathbf{G}[j]$, is

Fractional delay-Dopplers are considered in the analysis in Appendix A.

given by $\mathbf{G}[j] = [\hat{g}((k-0)_N, (l-0)_M) \quad \hat{g}((k-1)_N, (l-1)_M) \quad \cdots \hat{g}((k-N-1)_N, (l-M-1)_M)]$, where $\hat{g}(k,l)$ denotes the (k,l)th element of the $N \times M$ DD channel matrix, given by

$$\hat{g}(k,l) = \begin{cases} g_i' & \text{if } k = \beta_i, \ l = \alpha_i, \ i \in \{1, 2, \cdots, P\} \\ 0 & \text{otherwise.} \end{cases} \quad (7)$$

It can be seen from the above that the effective channel matrix $\mathbf{G}$ has only P non-zero entries in each row and column, i.e., there are only MNP non-zero elements in $\mathbf{G}$.

An alternate representation of input-output relation (6): In order to enable the diversity analysis, the input-output relation in (6) is written in an alternate form. Observing that the effective channel matrix $\mathbf{G}$ contains only P non-zero entries in each row and column, the vectorized input-output relation in (6) can be written in the following alternate form:

$$\mathbf{z}^T = \mathbf{g}'\mathbf{Y} + \mathbf{v}^T, \quad (8)$$

where $\mathbf{g}' \in \mathbb{C}^{1 \times P}$ is the channel vector with ith entry given by $g_i' = g_i e^{-j2\pi\nu_i\tau_i}$, $\mathbf{z}^T$, $\mathbf{v}^T \in \mathbb{C}^{1 \times MN}$, are the received signal vector and noise vector, respectively, and $\mathbf{Y} \in \mathbb{C}^{P \times MN}$ is the signal matrix with ith column $\mathbf{Y}[i]$, $i = k + Nl$, $k = 0, \cdots, N-1$, $l = 0, \cdots, M-1$, given by

$$\mathbf{Y}[i] = \begin{bmatrix} y_{(k-\beta_1)_N + N(l-\alpha_1)_M} \\ y_{(k-\beta_2)_N + N(l-\alpha_2)_M} \\ \vdots \\ y_{(k-\beta_P)_N + N(l-\alpha_P)_M} \end{bmatrix}. \quad (9)$$

The alternate representation in (8) is used to write the system model for MIMO-OTFS system in the following subsection.

A. MIMO-OTFS

The input-output relation in a MIMO-OTFS system with n_r receive antennas and n_t transmit antennas can be written as

$$\bar{\mathbf{z}} = \bar{\mathbf{G}}\bar{\mathbf{y}} + \bar{\mathbf{v}}, \quad (10)$$

which is written by concatenating n_r received signal vectors of the form (6) from n_r receive antennas, where $\bar{\mathbf{z}} = [\mathbf{z}_1^T \ \mathbf{z}_2^T \cdots \ \mathbf{z}_{n_r}^T]^T \in \mathbb{C}^{n_r MN \times 1}$, $\mathbf{z}_i$ being the received signal vector of the ith receive antenna, $\bar{\mathbf{y}} = [\mathbf{y}_1^T, \ \mathbf{y}_2^T \cdots \ \mathbf{y}_{n_t}^T]^T \in \mathbb{C}^{n_t MN \times 1}$, $\mathbf{y}_j$ being the transmit signal vector from the jth transmit antenna, $\bar{\mathbf{v}} = [\mathbf{v}_1^T, \ \mathbf{v}_2^T \cdots \ \mathbf{v}_{n_r}^T]^T \in \mathbb{C}^{n_r MN \times 1}$, $\mathbf{v}_i$ being the noise vector of the ith receive antenna, and the overall MIMO-OTFS channel matrix $\bar{\mathbf{G}} \in \mathbb{C}^{n_r MN \times n_t MN}$ is given by

$$\bar{\mathbf{G}} = \begin{bmatrix} \mathbf{G}_{11} & \cdots & \mathbf{G}_{1n_t} \\ \vdots & \ddots & \vdots \\ \mathbf{G}_{n_r 1} & \cdots & \mathbf{G}_{n_r n_t} \end{bmatrix}, \quad (11)$$

where $\mathbf{G}_{ij}$ denotes the $MN \times MN$ equivalent channel matrix between the ith receive antenna and jth transmit antenna.

An alternate input-output relation for MIMO-OTFS: We observe that in the overall equivalent MIMO-OTFS channel matrix $\bar{\mathbf{G}}$, each row contains only $n_t P$ unique non-zero elements and each column contains $n_r P$ unique non-zero
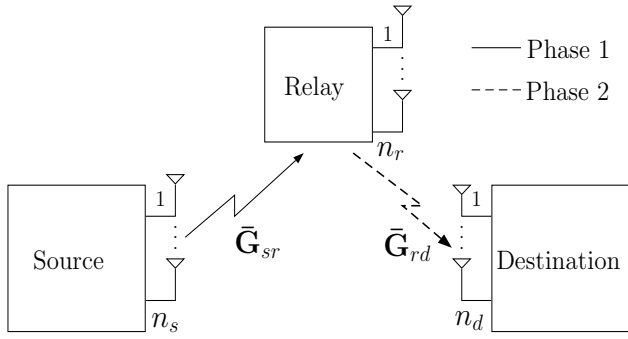
Fig. 1: MIMO-OTFS with decode-and-forward relaying scheme.

elements. Therefore, (10) can be written in the following alternate form:

$$\underbrace{\begin{bmatrix} \mathbf{z}_1^T \\ \vdots \\ \mathbf{z}_{n_r}^T \end{bmatrix}}_{\triangleq \tilde{\mathbf{Z}}} = \underbrace{\begin{bmatrix} \mathbf{g}_{11}' & \cdots & \mathbf{g}_{1n_t}' \\ \vdots & \ddots & \vdots \\ \mathbf{g}_{n_r 1}' & \cdots & \mathbf{g}_{n_r n_t}' \end{bmatrix}}_{\triangleq \tilde{\mathbf{G}}} \underbrace{\begin{bmatrix} \mathbf{Y}_1 \\ \vdots \\ \mathbf{Y}_{n_t} \end{bmatrix}}_{\triangleq \tilde{\mathbf{Y}}} + \underbrace{\begin{bmatrix} \mathbf{v}_1^T \\ \vdots \\ \mathbf{v}_{n_r}^T \end{bmatrix}}_{\triangleq \tilde{\mathbf{V}}}, \quad (12)$$

which can be written in a compact form as

$$\tilde{\mathbf{Z}} = \tilde{\mathbf{G}}\tilde{\mathbf{Y}} + \tilde{\mathbf{V}}, \quad (13)$$

where $\tilde{\mathbf{Z}} \in \mathbb{C}^{n_r \times MN}$ is the received signal matrix with $\mathbf{z}_i^T$ as the row corresponding to the ith receive antenna, $\tilde{\mathbf{G}} \in \mathbb{C}^{n_r \times n_t P}$ is the channel matrix with $\mathbf{g}_{ij}' \in \mathbb{C}^{1 \times P}$ being the row containing the unique non-zero entries of the channel matrix $\mathbf{G}_{ij}$, $\hat{\mathbf{Y}} \in \mathbb{C}^{n_t P \times MN}$ is the transmit symbol matrix with $\mathbf{Y}_j \in \mathbb{C}^{P \times MN}$ being the transmit signal matrix from the jth transmit antenna, and $\tilde{\mathbf{V}} \in \mathbb{C}^{n_r \times MN}$ is the noise matrix.

B. Decode-and-forward relaying

In this subsection, we present the MIMO-OTFS system model with DaF relaying. The block diagram of MIMO-OTFS system with DaF relaying is shown in Fig. 1. There is no direct link between source and destination, signifying a scenario where direct path between source and destination is blocked. Communication happens in two hops − source to relay in first hop and relay to destination in second hop. Let n_s and n_r denote the number of transmit antennas at the source (S) and relay (R), respectively, and n_d denote the number of receive antennas at the destination (D). Here, n_s and n_r are kept same to ensure same transmit signal dimensions at S and R. The number of receive antennas at R is considered to be the same as n_r so that the same antennas can be used for both reception and transmission at R. Also, n_d is taken to be greater than or equal to n_r so that the system is not under-determined. Transmission occurs in two phases. In the first phase, the source node transmits information to the relay. The received signal at the relay is given by

$$\bar{\mathbf{z}}_{sr} = \bar{\mathbf{G}}_{sr}\bar{\mathbf{y}} + \bar{\mathbf{v}}_{sr}, \quad (14)$$

where $\bar{\mathbf{z}}_{sr}, \bar{\mathbf{v}}_{sr} \in \mathbb{C}^{n_r MN \times 1}$ are the received signal vector and noise vector at the relay, $\bar{\mathbf{G}}_{sr} \in \mathbb{C}^{n_r MN \times n_s MN}$ is the equivalent channel matrix between source and relay, $\bar{\mathbf{y}} \in \mathbb{C}^{n_s MN \times 1}$

is the transmit signal vector from the source. During the second phase, the relay forwards the decoded information to the destination. The received signal at the destination is given by

$$\bar{\mathbf{z}}_{rd} = \bar{\mathbf{G}}_{rd}\bar{\hat{\mathbf{y}}} + \bar{\mathbf{v}}_{rd}, \quad (15)$$

where $\bar{\mathbf{z}}_{rd}, \bar{\mathbf{v}}_{rd} \in \mathbb{C}^{n_d MN \times 1}$ are the received signal vector and noise vector at the destination, $\bar{\mathbf{G}}_{rd} \in \mathbb{C}^{n_d MN \times n_r MN}$ is the equivalent channel matrix between relay and destination, and $\bar{\hat{\mathbf{y}}} \in \mathbb{C}^{n_r MN \times 1}$ is the transmit signal vector from relay.

Alternate form for MIMO-OTFS with DaF: The input-output relation in (14) and (15) can be written in an alternate form based on (12). The received signal at the relay in the first phase can be written as

$$\tilde{\mathbf{Z}}_{sr} = \tilde{\mathbf{G}}_{sr}\tilde{\mathbf{Y}} + \tilde{\mathbf{V}}_{sr}, \quad (16)$$

where $\tilde{\mathbf{Z}}_{sr}, \tilde{\mathbf{V}}_{sr} \in \mathbb{C}^{n_r \times MN}$, $\tilde{\mathbf{G}}_{sr} \in \mathbb{C}^{n_r \times n_s P_{sr}}$, and $\tilde{\mathbf{Y}} \in \mathbb{C}^{n_s P_{sr} \times MN}$. Likewise, the received signal at the destination in the second phase can be written as

$$\tilde{\mathbf{Z}}_{rd} = \tilde{\mathbf{G}}_{rd}\tilde{\hat{\mathbf{Y}}} + \tilde{\mathbf{V}}_{rd}, \quad (17)$$

where $\tilde{\mathbf{Z}}_{rd}, \tilde{\mathbf{V}}_{rd} \in \mathbb{C}^{n_d \times MN}$, $\tilde{\mathbf{G}}_{rd} \in \mathbb{C}^{n_d \times n_r P_{rd}}$, $\tilde{\hat{\mathbf{Y}}} \in \mathbb{C}^{n_r P_{rd} \times MN}$, P_{sr} and P_{rd} are the number of resolvable DD domain paths between S-to-R and R-to-D links, respectively.

C. OTFS with phase rotation

Phase rotation (PR) in OTFS is performed by pre-multiplying the OTFS vector $\mathbf{y}$ by a PR matrix $\boldsymbol{\Theta}$, given by $\boldsymbol{\Theta} = \text{diag}\{e^{j\frac{q}{MN}}\}$, $q = 0, \cdots, MN - 1$. Therefore, $\mathbf{y}' = \boldsymbol{\Theta}\mathbf{y}$ is the phase rotated OTFS transmit vector. In [6], it was shown that SISO-OTFS with the above PR operation is capable of achieving full possible diversity in the DD domain when $e^{j\frac{q}{MN}}$, $q = 0, 1, \cdots, MN - 1$ are transcendental numbers and $\frac{q}{MN}$ are real, distinct, and algebraic. We will analyze MIMO-OTFS without and with PR in the considered relaying scheme.

III. PERFORMANCE ANALYSIS

In this section, we analyze the diversity performance of MIMO-OTFS with DaF relaying. Maximum likelihood (ML) detection is considered at the relay and the destination. The minimum rank of difference matrices in a given system plays a key role in determining the diversity performance of the system. Therefore, we first characterize the minimum rank in the considered relaying system.

A. Minimum rank on various links with relaying

In the S-to-R link, let $\tilde{\mathbf{Y}}_i$ and $\tilde{\mathbf{Y}}_j$ be two distinct MIMO-OTFS symbol matrices without PR defined in (16), and $\tilde{\mathbf{Y}}_i'$ and $\tilde{\mathbf{Y}}_j'$ be two such matrices with PR. As in [6], the minimum ranks of $(\tilde{\mathbf{Y}}_i - \tilde{\mathbf{Y}}_j)$ and $(\tilde{\mathbf{Y}}_i' - \tilde{\mathbf{Y}}_j')$ on the S-to-R link for MIMO-OTFS are 1 and P_{sr}, respectively. Now, consider the R-to-D link. Note that the detected vector at the relay (error-free or erroneous) belongs to the same OTFS signal set at the source. In the R-to-D link, let $\tilde{\hat{\mathbf{Y}}}_i$ and $\tilde{\hat{\mathbf{Y}}}_j$ denote two distinct symbol matrices without PR and $\tilde{\hat{\mathbf{Y}}}_i'$, $\tilde{\hat{\mathbf{Y}}}_j'$ be two such matrices with PR. We are interested in the minimum rank

of the difference matrix $(\tilde{\mathbf{Y}}_i - \tilde{\mathbf{Y}}_j)$, $\forall i, j$. To find that, we note that the elements of the symbol matrices $\tilde{\mathbf{Y}}_i$ and $\tilde{\mathbf{Y}}_j$ are symbols from the modulation alphabet $\mathbb{A}$. Without PR, the set of all the possible symbol matrices will include the matrix $a\mathbf{1}_{n_r P_{rd} \times MN}$, where $a \in \mathbb{A}$. Now, considering the two distinct matrices to be $\tilde{\mathbf{Y}}_i = a\mathbf{1}_{n_r P_{rd} \times MN}$ and $\tilde{\mathbf{Y}}_j = a'\mathbf{1}_{n_r P_{rd} \times MN}$, $a \neq a'$, the difference matrix is given by $(a - a')\mathbf{1}_{n_r P_{rd} \times MN}$ whose all elements will be the same. Therefore, its rank is one which is the minimum rank.

Next, with PR, letting $\tilde{\boldsymbol{\Delta}}'_{ij} = (\tilde{\mathbf{Y}}'_i - \tilde{\mathbf{Y}}'_j)$, we have

$$\tilde{\boldsymbol{\Delta}}'_{ij} = \begin{bmatrix} \boldsymbol{\Delta}'_{1,ij} \\ \vdots \\ \boldsymbol{\Delta}'_{n_r,ij} \end{bmatrix}, \tag{18}$$

where $\boldsymbol{\Delta}'_{m,ij} = \hat{\mathbf{Y}}'_{m,i} - \hat{\mathbf{Y}}'_{m,j}$ and $\hat{\mathbf{Y}}'_{m,i}$ and $\hat{\mathbf{Y}}'_{m,j}$ are the transmitted symbol matrices from the mth antenna. The minimum rank of $\boldsymbol{\Delta}'_{m,ij}$ is P_{rd} for all $m = 1, \cdots, n_r$. Therefore, the minimum rank of $(\tilde{\mathbf{Y}}'_i - \tilde{\mathbf{Y}}'_j)$ is P_{rd}.

B. Diversity analysis

In this subsection, we analyze the diversity performance of MIMO-OTFS with DaF relaying. We bound the bit error rate using pairwise error probability (PEP) expression to quantify the diversity order. Let U denote the error event on the S-to-R link with probability $P_b(S \rightarrow R)$, and V denote the error event on the R-to-D link with probability $P_b(R \rightarrow D)$. With DaF relaying, U and V constitute independent events. Additionally, their intersection $W = U \cap V$ represents the errors in both links with probability $P_b(S \rightarrow R)P_b(R \rightarrow D)$. At the destination, W may not contain any erroneous bits because some erroneous bits found in S-to-R links may be corrected if they appear in R-to-D links as well. Therefore, the total end-to-end error can be expressed as $U + V - (1 + \delta)W$, where δ ($0 \leq \delta \leq 1$) is determined by the modulation scheme used. In general, however, both $P_b(S \rightarrow R)$ and $P_b(R \rightarrow D)$ are quite small, so the probability of $W = P_b(S \rightarrow R)P_b(R \rightarrow D)$ can be neglected. As a result, the bit error probability of the end-to-end system can be approximated by [12]

$$P_b \approx P_b(S \rightarrow R) + P_b(R \rightarrow D). \tag{19}$$

Further, $P_b(S \rightarrow R)$ and $P_b(R \rightarrow D)$ are upper bounded by the union bound based on PEP. Assume ML detection and perfect DD channel state information at R and D. On the S-to-D link, the probability $P_b(S \rightarrow R)$ can be bounded as

$$P_b(S \rightarrow R) \leq C_1 \sum_i \sum_{j,j \neq i} d_H(\bar{\mathbf{y}}_i, \bar{\mathbf{y}}_j) P_{S \rightarrow R}(\tilde{\mathbf{Y}}_i \rightarrow \tilde{\mathbf{Y}}_j), \tag{20}$$

where $C_1 = \frac{1}{Ln_s MN \log_2 |\mathbb{A}|}$, $L = |\mathbb{A}^{n_s MN}|$, $d_H(\bar{\mathbf{y}}_i, \bar{\mathbf{y}}_j)$ is number of bits in $\bar{\mathbf{y}}_i$ which differ from those in $\bar{\mathbf{y}}_j$, and

$P_{S \rightarrow R}(\tilde{\mathbf{Y}}_i \rightarrow \tilde{\mathbf{Y}}_j)$ is the average PEP between the symbol matrices $\tilde{\mathbf{Y}}_i$ and $\tilde{\mathbf{Y}}_j$ given by

$$P_{S \rightarrow R}(\tilde{\mathbf{Y}}_i \rightarrow \tilde{\mathbf{Y}}_j) = \mathbb{E}_{\tilde{\mathbf{G}}_{sr}}\left\{ Q\left(\sqrt{\frac{\|\tilde{\mathbf{G}}_{sr}(\tilde{\mathbf{Y}}_i - \tilde{\mathbf{Y}}_j)\|^2}{2N_0}} \right) \right\}, \tag{21}$$

where the averaging is over the distribution of $\tilde{\mathbf{G}}_{sr}$. We have normalized the entries of $\tilde{\mathbf{Y}}$ so that the average energy per symbol time is one and the signal-to-noise ratio (SNR) is given by $\gamma_s = 1/N_0$. Upper bounding (21) using Chernoff bound, we get

$$P_{S \rightarrow R}(\tilde{\mathbf{Y}}_i \rightarrow \tilde{\mathbf{Y}}_j) \leq \mathbb{E}_{\tilde{\mathbf{G}}_{sr}}\left\{ \exp\left(\frac{-\gamma_s \|\tilde{\mathbf{G}}_{sr}(\tilde{\mathbf{Y}}_i - \tilde{\mathbf{Y}}_j)\|^2}{4} \right) \right\}, \tag{22}$$

Carrying out the averaging, we get [6]

$$P_{S \rightarrow R}(\tilde{\mathbf{Y}}_i \rightarrow \tilde{\mathbf{Y}}_j) \leq \left(\frac{1}{\prod_{l=1}^{r_{sr}}(1 + \frac{\gamma_s \lambda_{sr}^{lij}}{4P_{sr}})} \right)^{n_r}, \tag{23}$$

where r_{sr} and λ_{sr}^{lij} are the rank and eigenvalue of $(\tilde{\mathbf{Y}}_i - \tilde{\mathbf{Y}}_j)(\tilde{\mathbf{Y}}_i - \tilde{\mathbf{Y}}_j)^H$ in the S-to-R link, respectively. Next, on the R-to-D link, $P_b(R \rightarrow D)$ is bounded as

$$P_b(R \rightarrow D) \leq C_2 \sum_i \sum_{j,j \neq i} d_H(\bar{\tilde{\mathbf{y}}}_i, \bar{\tilde{\mathbf{y}}}_j) P_{R \rightarrow D}(\tilde{\tilde{\mathbf{Y}}}_i \rightarrow \tilde{\tilde{\mathbf{Y}}}_j), \tag{24}$$

where $C_2 = \frac{1}{Ln_r MN \log_2 |\mathbb{A}|}$ and $P_{R \rightarrow D}(\tilde{\tilde{\mathbf{Y}}}_i \rightarrow \tilde{\tilde{\mathbf{Y}}}_j)$ is the PEP between symbol matrices $\hat{\tilde{\mathbf{Y}}}_i$ and $\hat{\tilde{\mathbf{Y}}}_j$. Following similar steps from (21)-(23), we obtain

$$P_{R \rightarrow D}(\tilde{\tilde{\mathbf{Y}}}_i \rightarrow \tilde{\tilde{\mathbf{Y}}}_j) \leq \left(\frac{1}{\prod_{l=1}^{r_{rd}}(1 + \frac{\gamma_r \lambda_{rd}^{lij}}{4P_{rd}})} \right)^{n_d}, \tag{25}$$

where γ_r is the normalized SNR on the R-to-D link. From (19), (23), (25), we have

$$P_b \leq C_1 \sum_i \sum_{j,j \neq i} d_H(\bar{\mathbf{y}}_i, \bar{\mathbf{y}}_j) \left(\frac{1}{\prod_{l=1}^{r_{sr}}(1 + \frac{\gamma_s \lambda_{sr}^{lij}}{4P_{sr}})} \right)^{n_r}$$
$$+ C_2 \sum_i \sum_{j,j \neq i} d_H(\bar{\tilde{\mathbf{y}}}_i, \bar{\tilde{\mathbf{y}}}_j) \left(\frac{1}{\prod_{l=1}^{r_{rd}}(1 + \frac{\gamma_r \lambda_{rd}^{lij}}{4P_{rd}})} \right)^{n_d}. \tag{26}$$

At high SNRs, using the approximation $(1 + \frac{\gamma_s}{4P_{sr}}) \approx (\frac{\gamma_s}{4P_{sr}})$ and $(1 + \frac{\gamma_r}{4P_{rd}}) \approx (\frac{\gamma_r}{4P_{rd}})$, (26) can be written as

$$P_b \leq \tilde{C}_1 \gamma_s^{-n_r r_{sr}} + \tilde{C}_2 \gamma_r^{-n_d r_{rd}}, \tag{27}$$

where $\tilde{C}_1 = C_1 \sum_i \sum_{j,j \neq i} d_H(\bar{\mathbf{y}}_i, \bar{\mathbf{y}}_j) \left(\prod_{l=1}^{r_{sr}}(\frac{\lambda_{sr}^{lij}}{4P_{sr}}) \right)^{-n_r}$ and $\tilde{C}_2 = C_2 \sum_i \sum_{j,j \neq i} d_H(\bar{\tilde{\mathbf{y}}}_i, \bar{\tilde{\mathbf{y}}}_j) \left(\prod_{l=1}^{r_{rd}}(\frac{\lambda_{rd}^{lij}}{4P_{rd}}) \right)^{-n_d}$ are appropriately defined constants. For equal power allocation at S and R, we have $\gamma_s = \gamma_r = \gamma$. So, (27) becomes

$$P_b \leq \tilde{C}_1 \gamma^{-n_r r_{sr}} + \tilde{C}_2 \gamma^{-n_d r_{rd}}. \tag{28}$$

For $n_r r_{sr} > n_d r_{rd}$, at high SNRs, the second term in (28) dominates. Therefore, (28) can be written as

Parameter	Value
Carrier frequency, f_c	4 GHz
Subcarrier spacing, Δf	3.75 kHz
DD profile (τ_i, ν_i) for 1 DD path	$(\frac{1}{M\Delta f}, \frac{1}{NT})$
DD profile (τ_i, ν_i) for 2 DD paths, for $M = 2, 4$, $N = 2$	$(0, 0), (\frac{1}{M\Delta f}, \frac{1}{NT})$
DD profile (τ_i, ν_i) for 4 DD paths, for $M = 2, 4$, $N = 2$	$(0, 0), (0, \frac{1}{NT})$, $(\frac{1}{M\Delta f}, 0), (\frac{1}{M\Delta f}, \frac{1}{NT})$
Maximum speed	506.2 kmph
Modulation	BPSK, QPSK

TABLE I: Simulation parameters.

$$P_b \leq \tilde{C}_2 \gamma^{-n_d r_{rd}}. \tag{29}$$

Therefore, the diversity order is $n_d r_{rd}$. On the other hand, for $n_r r_{sr} < n_d r_{rd}$, the first term in (28) dominates and the diversity order is $n_r r_{sr}$. Combining these two, the diversity order can be written as $\min\{n_r r_{sr}, n_d r_{rd}\}$. This leads to the following diversity orders.

- The achieved diversity order in MIMO-OTFS system wtih DaF relaying without PR is $\min\{n_r, n_d\} = n_r$, since the minimum ranks are $r_{sr} = 1$, $r_{rd} = 1$.
- The achieved diversity order in MIMO-OTFS system with DaF relaying with PR is $\min\{n_r P_{sr}, n_d P_{rd}\}$, since the minimum ranks are $r_{sr} = P_{sr}$, $r_{rd} = P_{rd}$.

IV. RESULTS AND DISCUSSIONS

In this section, we present simulation results on the bit error performance which validate the diversity analysis presented in the previous section. The bit error rate (BER) performance of the considered MIMO-OTFS system with DaF relaying are evaluated with and without PR. The number of DD paths considered on the various links are 1, 2, and 4. Table I shows the system parameters used in the simulations.

SISO-OTFS with DaF (without PR): Figure 2 shows the simulated BER of SISO-OTFS ($n_s = n_r = n_d = 1$) with DaF and without PR for $M = N = 2$, $P_{sr} = 2, 4$, and $P_{rd} = 2$. Table I provides the DD channel profile considered for the considered frame size and number of DD paths. The DD channel model is given in (3). Additional simulation parameters are presented in Table I. From Fig. 2, it is observed that the diversity order without PR is one, i.e., there is one order of improvement in BER for every 10 dB increase in SNR in the high-SNR regime. This observed diversity of one is in conformance with the analysis in Sec. III-B, where the diversity order without PR is predicted to be n_r, which in this case is 1. Also, the BER upper bounds plotted in the same figure are very close to the simulated BERs, validating the analysis.

SISO-OTFS with DaF (with PR): Figure 3 shows the simulated BER of SISO-OTFS with DaF and with PR for $M = 4$, $N = 2$, $P_{sr} = 1, 2, 4$, and $P_{rd} = 1, 2$. It is observed that the system with $P_{sr} = 1$ and $P_{rd} = 2$ achieves a diversity slope of one. This is in agreement with the analytically predicted diversity, which is $\min\{n_r P_{sr}, n_d P_{rd}\} = \min\{1, 2\} = 1$. It is also seen that the system with $P_{sr} = 2$ and $P_{rd} = 2$ achieves
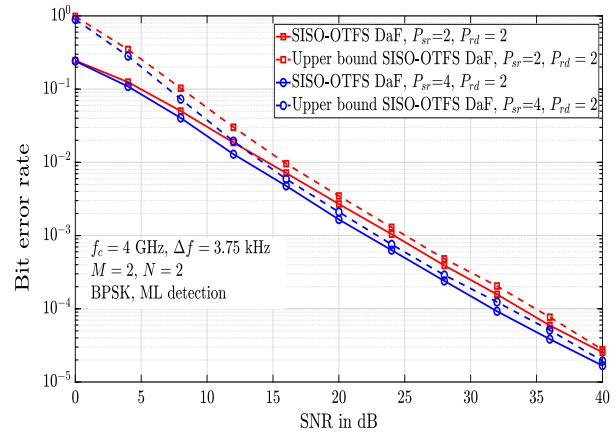

Fig. 2: Bit error rate performance of SISO-OTFS with DaF without PR for $M = N = 2$, $P_{sr} = 2, 4$, $P_{rd} = 2$.
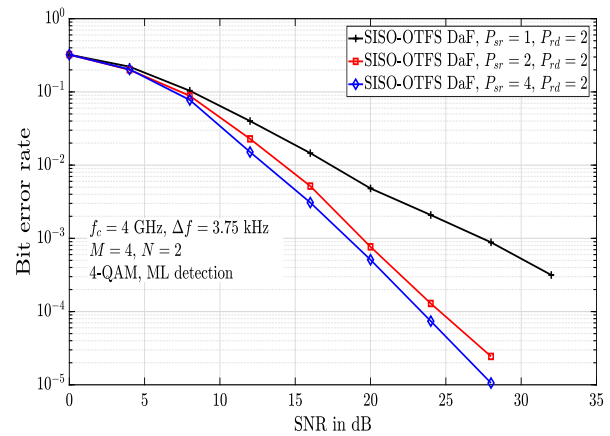

Fig. 3: Bit error rate performance of SISO-OTFS with DaF with PR for $M = 4$, $N = 2$, $P_{sr} = 1, 2, 4$, $P_{rd} = 2$.

a diversity slope of two, which is also in agreement with the analytically obtained diversity of $\min\{n_r P_{sr}, n_d P_{rd}\} = \min\{2, 2\} = 2$. Likewise, the system with $P_{sr} = 4$ and $P_{rd} = 2$ also achieves a diversity slope of two, conforming to the analytical diversity of $\min\{n_r P_{sr}, n_d P_{rd}\} = \min\{4, 2\} = 2$.

MIMO-OTFS with DaF (with and without PR): Figure 4 shows the simulated BER of MIMO-OTFS with DaF for $n_s = n_r = 2$, $n_d = 2, 3$, $M = N = 2$, $P_{sr} = 1, 2$, and $P_{rd} = 1, 2$. For the system without PR, for $n_s = n_r = n_d = 2$, $P_{sr} = 1$, and $P_{rd} = 2$, the observed diversity slope is two, which is the same as the analytical diversity of $n_r(= 2)$. For the same system with PR, the observed diversity slope is also two. This is because the analysis predicts the diversity to be $\min\{n_r P_{sr}, n_d P_{rd}\} = \min\{2, 4\} = 2$. That is, the link with the lower minimum rank dominates the overall diversity slope. In this case, the minimum ranks of S-to-R and R-to-D links are $P_{sr}(= 1)$ and $P_{rd}(= 2)$, respectively. Similarly, the system with $n_s = n_r = 2$, $n_d = 3$, $P_{sr} = 2$, $P_{rd} = 1$ and without PR shows a diversity slope of two (analytical diversity is also $n_r(= 2)$). For the same system with PR, the observed diversity slope is three, as per $\min\{n_r P_{sr}, n_d P_{rd}\} = \min\{4, 3\} = 3$.
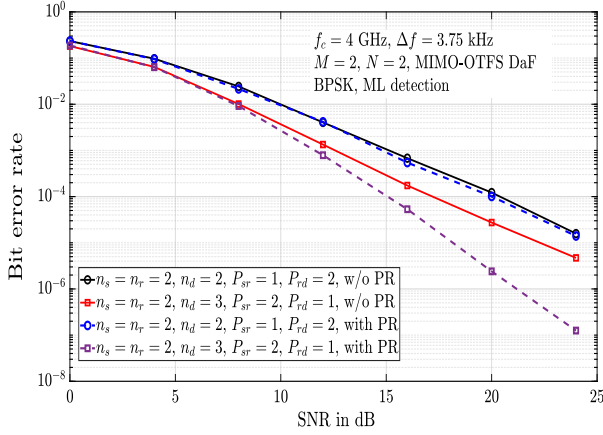
Fig. 4: Bit error rate performance of MIMO-OTFS with DaF and with and without PR for $M = N = 2$, $P_{sr} = 1, 2$, $P_{rd} = 1, 2$.

A. Analysis and results for fractional delay-Dopplers

The results presented above are for integer delays and Dopplers. The diversity analysis for fractional DDs is presented in Appendix A. In this subsection, we present the simulated BER performance with fractional delays and Dopplers. First, we validate the analytical diversity results for small frame sizes and ML detection, and present simulated BER results for large frame sizes with minimum mean square error (MMSE) detection. A performance comparison between MIMO-OTFS and MIMO-OFDM is also presented.

Results for small values of M and N: Figure 5 shows the simulated bit error performance of MIMO-OTFS with DaF relaying without PR for $n_s = n_r = n_d = 2$, $M = N = 2$, $P_{sr} = 2$, and $P_{rd} = 2, 4$. The Doppler corresponding to the ith channel tap is generated using $\nu_i = \nu_{\max} \cos(\theta_i)$, where $\nu_{\max}$ is the maximum Doppler, and θ_i is uniformly distributed over $[-\pi, \pi]$. The delay corresponding to ith channel tap is generated as uniformly distributed over $[0, (M - 1)T_s]$, where $T_s = 1/(M\Delta f)$ and Δf is the subcarrier spacing. Exponential power delay profile and Jakes Doppler spectrum are considered. ML detection is used. The diversity order for MIMO-OTFS with DaF from the analysis is $n_r = 2$ and the observed diversity order from simulation is also 2 validating the analysis.

Results for large values of M and N: Figure 6 shows a performance comparison between MIMO-OTFS and MIMO-OFDM with DaF for large values of M and N and rectangular pulse, considering system parameters according to the IEEE 802.11p standard [15]. The carrier frequency and subcarrier spacing are 5.9 GHz and 0.156 MHz, respectively. A frame size of $M = 64$, $N = 12$, number of paths $P_{sr} = P_{rd} = 8$, fractional DDs with a maximum speed of 220 km/h (corresponding maximum Doppler of 1.2 kHz), and BPSK modulation are considered. Since ML detection is prohibitively complex for large values for M and N, MMSE detection is used. From Fig. 6, we observe that the performance of MIMO-OTFS is significantly better than the MIMO-OFDM system.
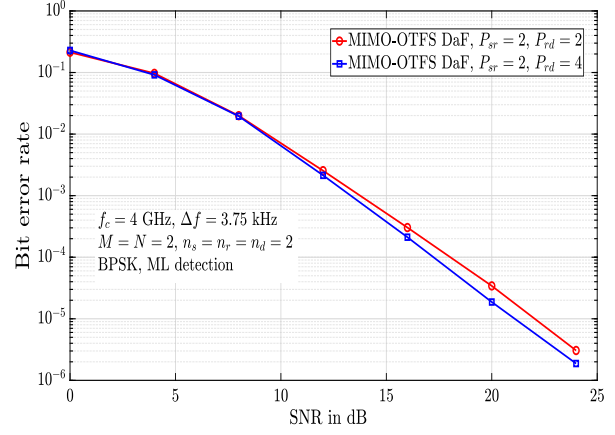

Fig. 5: Bit error rate performance of MIMO-OTFS without PR for $M = N = 2$, $P_{sr} = 2$, $P_{rd} = 2, 4$ and fractional DDs.
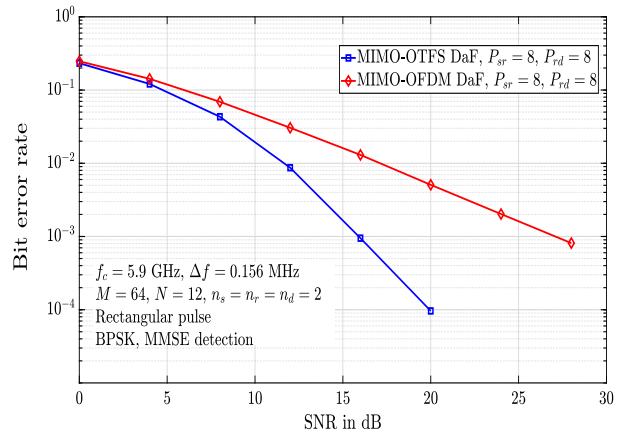

Fig. 6: BER performance comparison between MIMO-OTFS and MIMO-OFDM with relaying for $M = 64$, $N = 12$, $P_{sr} = P_{rd} = 8$, $n_s = n_r = n_d = 2$.

For example, at a BER of 10^{-3}, MIMO-OTFS with DaF has a gain of about 10 dB compared to MIMO-OFDM with DaF.

V. CONCLUSIONS

In this work, we investigated the performance of MIMO-OTFS systems with decode and forward relaying. We considered MIMO-OTFS with a single relay to aid communication between the transmitter and receiver. We derived a closed-form expression for the end-to-end PEP in this system and quantified the achieved asymptotic diversity order with and without PR. Simulation results were shown to validate the analytically derived diversity orders. Future work may consider diversity analysis of MIMO-OTFS with DaF relaying using practical pulse shapes. Optimal power allocation schemes for the source and relay nodes can also be explored. Multiple relay nodes with relay selection and the effect of inter-node distances on the achieved diversity performance can also be analyzed as future work.

APPENDIX A
ANALYSIS FOR FRACTIONAL DELAYS AND DOPPLERS

$$\mathbf{Y}[i] = \begin{bmatrix} \sum_{q=0}^{M-1} \sum_{q'=0}^{N-1} \left(\frac{e^{j2\pi(-q-a_1)}-1}{Me^{j\frac{2\pi}{M}(-q-a_1)}-M} \right) \left(\frac{e^{-j2\pi(-q'-b_1)}-1}{Ne^{-j\frac{2\pi}{N}(-q'-b_1)}-N} \right) y[(k-\beta_1+q')_N, (l-\alpha_1+q)_M] \\ \sum_{q=0}^{M-1} \sum_{q'=0}^{N-1} \left(\frac{e^{j2\pi(-q-a_2)}-1}{Me^{j\frac{2\pi}{M}(-q-a_2)}-M} \right) \left(\frac{e^{-j2\pi(-q'-b_2)}-1}{Ne^{-j\frac{2\pi}{N}(-q'-b_2)}-N} \right) y[(k-\beta_2+q')_N, (l-\alpha_2+q)_M] \\ \vdots \\ \sum_{q=0}^{M-1} \sum_{q'=0}^{N-1} \left(\frac{e^{j2\pi(-q-a_P)}-1}{Me^{j\frac{2\pi}{M}(-q-a_P)}-M} \right) \left(\frac{e^{-j2\pi(-q'-b_P)}-1}{Ne^{-j\frac{2\pi}{N}(-q'-b_P)}-N} \right) y[(k-\beta_P+q')_N, (l-\alpha_P+q)_M] \end{bmatrix}. \tag{30}$$

In this appendix, we present the analysis for the case of fractional delays and Dopplers.

Input-output relation with fractional delays and Dopplers: Consider the delays and Dopplers in the DD channel model defined in (3) to be fractional, where

$$\tau_i = \frac{\alpha_i + a_i}{M\Delta f}, \quad \nu_i = \frac{\beta_i + b_i}{NT}, \tag{31}$$

$\alpha_i = [\tau_i M\Delta f]^\odot$, $\beta_i = [\nu_i NT]^\odot$, $[.]^\odot$ denotes the rounding operator (nearest integer), and a_i, b_i are fractional delays and Dopplers satisfying $-\frac{1}{2} < a_i, b_i \le \frac{1}{2}$. With fractional DDs and rectangular window functions, the DD channel can be expressed as [6]

$$g(\tau, \nu) = \sum_{i=1}^{P} g_i e^{-j2\pi\tau_i\nu_i} \mathcal{G}(\nu, \nu_i) \mathcal{F}(\tau, \tau_i), \tag{32}$$

where $\mathcal{G}(\nu, \nu_i) \triangleq \sum_{n'=0}^{N-1} e^{-j2\pi(\nu-\nu_i)n'T}$, and $\mathcal{F}(\tau, \tau_i) \triangleq \sum_{m'=0}^{M-1} e^{j2\pi(\tau-\tau_i)m'\Delta f}$. The input-output relation with fractional DD can be written as [6]

$$\begin{aligned} z[k,l] = \sum_{i=1}^{P} \sum_{q=0}^{M-1} \sum_{q'=0}^{N-1} & \left(\frac{e^{j2\pi(-q-a_i)}-1}{Me^{j\frac{2\pi}{M}(-q-a_i)}-M} \right) \\ & \cdot \left(\frac{e^{-j2\pi(-q'-b_i)}-1}{Ne^{-j\frac{2\pi}{N}(-q'-b_i)}-N} \right) g_i e^{-j2\pi\tau_i\nu_i} \\ & \cdot y[(k-\beta_i+q')_N, (l-\alpha_i+q)_M]. \end{aligned} \tag{33}$$

The input-output relation (33) can be written in a vectorized form as

$$\mathbf{z} = \mathbf{G}\mathbf{y} + \mathbf{v}, \tag{34}$$

where $\mathbf{z} \in \mathbb{C}^{MN \times 1}$ is the received signal vector, $\mathbf{y} \in \mathbb{C}^{MN \times 1}$ is the transmit signal vector, $\mathbf{G} \in \mathbb{C}^{MN \times MN}$ is the equivalent channel matrix, and $\mathbf{v} \in \mathbb{C}^{MN \times 1}$ is the noise vector. The vectorized input-output relation in (34) can be written in alternate form as

$$\mathbf{z}^T = \mathbf{g}'\mathbf{Y} + \mathbf{v}^T, \tag{35}$$

where $\mathbf{z}^T$ is $1 \times MN$ received vector, $\mathbf{g}' \in \mathbb{C}^{1 \times P}$ is vector having its ith entry as $g_i e^{-j2\pi\tau_i\nu_i}$, $\mathbf{Y} \in \mathbb{C}^{P \times MN}$ is symbol matrix with its ith column ($i = k+Nl, i = 0, 1, \cdots, MN-1$), and $\mathbf{Y}[i]$ is given by in (30) at the top of the page. The input-output relation given in (34), (35) can be extended to MIMO-OTFS with DaF defined in Sec. II-B.

Diversity of MIMO-OTFS DaF: Using the alternate form defined in (16) and (17), and following the steps from (19)-(27), BER upper bound is given by

$$P_b \le \tilde{C}_1 \gamma^{-n_r r_{sr}} + \tilde{C}_2 \gamma^{-n_d r_{rd}}, \tag{36}$$

where $\tilde{C}_1$ and $\tilde{C}_2$ are appropriately defined constants. Using similar arguments made in Sec. III-B, the diversity order is obtained as $\min\{n_r r_{sr}, n_d r_{rd}\}$. For MIMO-OTFS without PR, the achieved diversity order is $\min\{n_r, n_d\} = n_r$, since the minimum ranks are $r_{sr} = 1$ and $r_{rd} = 1$.

REFERENCES

[1] R. Hadani *et al.,* "Orthogonal time frequency space modulation," *Proc. IEEE WCNC'2017*, pp. 1-7, Mar. 2017.

[2] S. S. Das, R. Prasad, *OTFS: Orthogonal Time Frequency Space Modulation - A Waveform for 6G*, River Publishers, 2022.

[3] Y. Hong, T. Thaj, and E. Viterbo, *Delay-Doppler Communications: Principles and Applications*, Academic Press, 2022.

[4] P. Raviteja, K. T. Phan, Y. Hong, and E. Viterbo, "Interference cancellation and iterative detection for orthogonal time frequency space modulation," *IEEE Trans. Wireless Commun.*, vol. 17, no. 10, pp. 6501-6515, Aug. 2018.

[5] H. Qu, G. Liu, L. Zhang, S. Wen, and M. A. Imran, "Low-complexity symbol detection and interference cancellation for OTFS system," *IEEE Trans. Commun.*, vol. 69 no. 3, pp. 1524 - 1537, Dec. 2020.

[6] G. D. Surabhi, R. M. Augustine, and A. Chockalingam, "On the diversity of uncoded OTFS modulation in doubly-dispersive channels," *IEEE Trans. Wireless Commun.*, vol. 18, no. 6, pp. 3049-3063, Jun. 2019.

[7] P. Raviteja, Y. Hong , E. Viterbo , and E. Biglieri, "Effective diversity of OTFS modulation," *IEEE Wireless Commun. Lett.*, vol. 9, no. 2, pp. 249-253, Feb. 2020.

[8] V. S. Bhat, G. D. Surabhi, and A. Chockalingam, "Performance analysis of OTFS modulation with receive antenna selection," *IEEE Trans. Veh. Tech.*, vol. 70, no. 4, pp. 3382-3395, Apr. 2021.

[9] S. Li, J. Yuan, W. Yuan, Z. Wei, B. Bai, and D. W. K. Ng, "Performance analysis of coded OTFS systems over high-mobility channels," *IEEE Trans. Wireless Commun.*, vol. 20, no. 9, pp. 6033-6048, Sep. 2021.

[10] J. N. Laneman, D. N. C. Tse, and G. W. Wornell, "Cooperative diversity in wireless networks: Efficient protocols and outage behavior," *IEEE Trans. Inform. Theory*, vol. 50, no. 12, pp. 3062-3080, Dec. 2004.

[11] A. Nosratinia, T. E. Hunter, and A. Hedayat, "Cooperative communication in wireless networks," *IEEE Commun. Mag.*, vol. 42, no. 10, pp. 74-80, Oct. 2004.

[12] M. O. Hasna and M.-S. Alouini, "End-to-end performance of transmission systems with relays over Rayleigh-fading channels," *IEEE Trans. Wireless Commun.*, vol. 2, no. 6, pp. 1126-1131, Nov. 2003.

[13] Y. Khattabi and M. M. Matalgah, "Conventional and best-relay-selection cooperative protocols under nodes-mobility and imperfect-CSI impacts: BER performance," *Proc. IEEE WCNC'2015*, pp. 105-110, May 2015.

[14] N. Varshney and A. K. Jagannatham, "Performance analysis of MIMO-OSTBC based selective DF cooperative wireless system with node mobility and channel estimation errors," *Proc. Nat. Conf. Commun.*, pp. 1-6, IIT Guwahati, Mar. 2016.

[15] A. M. S. Abdelgader and W. Lenan, "The physical layer of the IEEE 802.11 p WAVE communication standard: the specifications and challenges," *Proc. World Congr. Eng. Comput. Sci.*, pp. 22-24, Oct. 2014.